Electronic energy loss for helium channeling in silicon

L. R. Logan, C. S. Murthy, and G. R. Srinivasan
Theoretical Modeling Department, IBM Semiconductor Research and Development Center, East Fishkill Facility, Hopewell Junction, New York 12533
(Received 29 April 1992; revised manuscript received 29 June 1992)

We present an analysis of the stopping power for helium in silicon taking into account the contributions due to different charge states. Our calculations include effects due to the nonuniformity of the target valence-electron density along specific crystallographic directions as well as the electron density of the projectile. In the present work attention is restricted to projectile velocities greater than or equal to the Bohr velocity in order to compare with existing experimental data. The method employs a dielectric-response formalism taken in the random-phase approximation coupled with energy-dependent population factors for the different charge states. It is demonstrated that the total stopping power obtained in the present work shows reasonable agreement with experiment.

PACS number(s): 34.50.Bw, 61.80.Mk

I. INTRODUCTION

The theory of electronic stopping of ions in solids has been a topic of interest for many decades. The problem is handled adequately at high energies by the Bethe [1] and Bloch [2] theories, where the particle is fully ionized. At lower energies the effects of the polarization charge of the particle become important. Various calculations, which have been quite successful, have been made for low-velocity ions (e.g., see [3,4,5]). The calculation of stopping power has been traditionally most difficult in the "intermediate"-energy region where it displays a maximum. There have been some calculations done, but generally good agreement with experiment is more difficult to obtain.

One important aspect of the intermediate-energy stopping power is its dependence on charge-state effects. It is primarily in this region where the greatest range of ionization states will exist. Azziz and co-workers [6] have performed calculations that have included the projectile charge density and demonstrated its importance on the stopping power for keV-range boron ions channeling in silicon. The issue of charge-state effects may also be addressed using the concept of effective charge. In particular, Brandt and Kitagawa [7] have defined an effective charge in terms of the ratio of the stopping powers for partially and fully ionized particles. This type of accounting for the charge distribution has been used in modeling low-energy boron implantation in silicon [8]. It should be pointed out, however, that the approach is based on the mean value of the ionization state. It does not give information on the relative contribution to the stopping power due to the different charge states. Furthermore, it is only with simplifying assumptions that the model can be applied, e.g., using the Thomas-Fermi model for the charge density accompanied with certain analytical approximations. This type of approximation is questionable for low-Z_1 ions.

The problem of charge-state effects has been addressed to various degrees in previous literature. Kaneko [9] reported calculations of stopping power for a helium beam in Al and also a H beam in Li (which can support the neutral H state). After calculating the stopping-power contributions from the various charge states, the results were superimposed using an empirical formula depending on the projectile energy. In doing so, reasonable agreement with experiment was observed with the best results occurring at energies $\gtrsim 1$ MeV/nucleon. More recently, Arnau *et al.* [10] performed a first-principles calculation showing the resulting stopping power for He in Al including the contributions from the individual charge-state species and also charge-changing events. Their results demonstrated good agreement with experiment with the region near the stopping-power maximum showing the largest discrepancy.

The present work deals with the case of helium channeling in silicon as an example. Since the available experimental data correspond to velocities at and above the Bohr velocity, we restrict our attention to velocities in that range. Additionally, our treatment of the problem includes effects due to the nonuniformity of the target valence-electron density, thus allowing for computation of stopping power along different crystallographic directions. In what follows, both the $\langle 111 \rangle$ and $\langle 110 \rangle$ axial directions in silicon are considered, for which comparison with experimental data is possible.

In order to calculate the stopping power for a specified charge state a dielectric-response formalism is used. The latter is taken in the random-phase approximation (RPA). There have been several previous treatments where energy loss has been determined using dielectric-response theory [11–16]. In the present work, however, the stopping power is obtained from direct integrations of the imaginary inverse dielectric function over frequency and wave vector without further approximations. The problem is defined in much the same way as by Burenkov, Komarov, and Kumakhov (BKK) [11], but the explicit evaluation of the relevant integrals permits an extension of the theory to lower energies. Also, our work takes into account the contributions due to the individual

charge states of the projectile to the total stopping power, whereas the work of BKK includes such effects indirectly through an effective-charge approximation [17].

Inside the material an electron will interact with the channeling helium nucleus through a screened Coulomb potential. Rogers, Graboske, and Harwood [18] have performed calculations of the number of bound states that exist with this interaction potential. Using this, Kaneko [9] has pointed out that helium cannot bind two electrons in a medium having $r_s < 4.92$ (here r_s represents the radial distance occupied by one electron in atomic units). For Si this condition is easily met and therefore we shall consider only the singly and doubly charged states of helium in Si.

In addition to being able to calculate the stopping power for a specified charge state, one must also know the relative populations of the charge states for the projectile. For this a simple statistical model is proposed using a Bohr electron-stripping criteria. For the case of helium, with only two charge states contributing, the relative proportion of each charge state is resolved and is used to superimpose the energy-loss results in a physically reasonable way.

The organization of the paper is as follows. In Sec. II some details of the theory are discussed. Section III contains some applications and comparisons with experimental results. Finally, in Sec. IV conclusions are presented.

II. THEORY

In this section a brief description of the theoretical framework is given. Much of the material describing the basic stopping-power formalism for fully ionized particles has been given by BKK [11] and various references therein. The interested reader is referred to that work for greater detail.

Consider a particle with nuclear charge Z_1 and N bound electrons traveling in the solid at a velocity $\mathbf{v}$. The projectile charge density as a function of position and time is given by

$$\rho_{ne}(\mathbf{r},t)=Z_1\delta(\mathbf{r}-\mathbf{v}t)-\rho_e(\mathbf{r}-\mathbf{v}t) , \tag{1}$$

where ρ_e denotes the electron charge density of the ion, the latter being normalized to N. It is straightforward to show that the stopping power S for a particle having a charge density given by (1) in a uniform electron gas is

$$S=-\frac{dE}{dx}=\frac{2}{\pi v^2}\int_0^\infty \frac{dq}{q}|\rho_{ne}(q)|^2 \times\int_0^{qv} d\omega\,\omega\,\mathrm{Im}\left[\frac{-1}{\epsilon(q,\omega)}\right] . \tag{2}$$

The function $\rho_{ne}(q)$ is the Fourier transform of the electron density given by Eq. (1) and $\epsilon(q,\omega)$ is the dielectric-response function depending on the wave vector q and frequency ω. The response function $\epsilon(q,\omega)$ describes the screening effects of the media on the field of the external charge and gives a dispersion relation for the collective excitations. The reader is referred to the book by Pines [19] for more information.

In the case where the medium has a nonuniform electronic structure, the stopping power for a fully ionized particle is given in [16]. When the latter is modified to include the electron density of the projectile, we have the result

$$-\frac{dE}{dx}(\mathbf{r})=\frac{e^2}{\pi^2 v}\int\frac{d^3q}{q^2}|\rho_{ne}(q)|^2 \times\int d\omega\,\omega\sum_{\mathbf{G}}\mathrm{Im}[K_{\mathbf{G},0}(\mathbf{q},\omega)] \times e^{i\mathbf{G}\cdot\mathbf{r}}\delta(\omega-\mathbf{q}\cdot\mathbf{v}) , \tag{3}$$

where the $K_{\mathbf{G},0}(\mathbf{q},\omega)$ are the inverse dielectric matrix elements [16,20], which satisfy the relation

$$\sum_{\mathbf{G}''}\epsilon_{\mathbf{G},\mathbf{G}''}(\mathbf{q},\omega)K_{\mathbf{G}'',\mathbf{G}'}(\mathbf{q},\omega)=\delta_{\mathbf{G},\mathbf{G}'} . \tag{4}$$

In the weak-binding limit a simple relation exists between the components of $K_{0,\mathbf{G}}$ and $\epsilon_{0,\mathbf{G}}$ as shown by Falk [20]:

$$K_{\mathbf{G},0}\simeq\delta_{\mathbf{G},0}-(1-\delta_{\mathbf{G},0})\frac{\epsilon_{0,\mathbf{G}}}{\epsilon_{0,0}} . \tag{5}$$

The $\epsilon_{0,0}$ in the above represents the usual response function defined for a uniform electron gas. For the dielectric matrix elements we use the results from the RPA [11],

$$\epsilon_{\mathbf{G},\mathbf{G}'}=\delta_{\mathbf{G},\mathbf{G}'}-\frac{4\pi e^2}{|\mathbf{q}+\mathbf{G}||\mathbf{q}+\mathbf{G}'|}\sum_{\mathbf{k},l,l'}M_{\mathbf{G}}(\mathbf{k}+\mathbf{q},l';\mathbf{k},l)M_{\mathbf{G}}(\mathbf{k}+\mathbf{q},l';\mathbf{k},l)^\dagger \times\Theta(k_F-k)\left\{\frac{1}{E_l(\mathbf{k})-E_{l'}(\mathbf{k}+\mathbf{q})-\hbar\omega+i\hbar\alpha}-\frac{1}{E_{l'}(\mathbf{k}+\mathbf{q})-E_l(\mathbf{k})-\hbar\omega+i\hbar\alpha}\right\} , \tag{6}$$

which correspond to the response of the system in the zero-temperature limit. The factor $M(\mathbf{k},l;\mathbf{q},l')$ represents the matrix element for the charge-density fluctuation given by

$$M_{\mathbf{G}}(\mathbf{k}+\mathbf{q},l';\mathbf{k},l)=\langle\mathbf{k}+\mathbf{q},l'|e^{i(\mathbf{q}+\mathbf{G})\cdot\mathbf{r}}|\mathbf{k},l\rangle . \tag{7}$$

The normal processes correspond to $\mathbf{G}=0$, whereas the umklapp processes correspond to $\mathbf{G}\neq0$.

Following Penn [21] and the subsequent work of other authors [11,15], it is assumed that the response function is insensitive to the $\mathbf{k}$ variation in the matrix elements shown in Eq. (7). Under these circumstances one may consider the latter to be replaced by their averages over $\mathbf{k}$ and hence they may be factored out of the integral. One may then deduce a simple relationship between the 0,0 and 0,G components of the dielectric matrix. The values of these matrix elements as a function of q may then be determined from the sum rule [22]

$$\int_0^\infty d\omega\,\omega\,\mathrm{Im}\epsilon_{\mathbf{G},0} = -\tfrac{1}{2}\pi\omega_p^2 f(\mathbf{G})\hat{\mathbf{e}}(\mathbf{q})\cdot\hat{\mathbf{e}}(\mathbf{q}+\mathbf{G}) , \quad (8)$$

where $\hat{\mathbf{e}}(\mathbf{q})$ is a unit vector in the direction of $\mathbf{q}$. The $f(\mathbf{G})$ are the Fourier components of the electron density in the crystal normalized to the uniform gas density [i.e., $f(0)=1$]. Using (8) it can be shown after some manipulations that the calculation of the stopping power may be reduced to the evaluation of the following formula:

$$-\frac{dE}{dx}(\mathbf{r}) = \sum_G S(\mathbf{G}) e^{i\mathbf{G}\cdot\mathbf{r}} , \quad (9a)$$

where

$$S(\mathbf{G}) = \frac{e^2}{\pi^2 v^2}\int_0^\infty \frac{dq}{q}|\rho_{ne}(q)|^2 \times \int_0^{qv} d\omega\,\omega\,\mathrm{Im}\left[\frac{-1}{\epsilon_{0,0}(q,\omega)}\right] f(\mathbf{G}) \times \int_0^{2\pi}\hat{\mathbf{e}}(\mathbf{q})\cdot\hat{\mathbf{e}}(\mathbf{q}+\mathbf{G})\,d\phi , \quad (9b)$$

subject to the condition $\mathbf{q}\cdot\mathbf{v}=\omega$.

In order to proceed further one must evaluate the real and imaginary components of the response function appearing in Eq. (9b). This requires that the energy wave-vector relation $E_l(\mathbf{k})$ be specified. In the present work a simplified electronic structure for semiconducting material is used following the work of Brandt and Reinheimer [15]. The model essentially consists of an electron gas supplemented with an energy gap E_g. The Fermi surface is considered to be located halfway in the forbidden gap, across which the single-particle excitations occur. Thus the energy wave-vector relationship is written as

$$E_l(\mathbf{k}) = \begin{cases} \dfrac{\hbar^2 k^2}{2m}, & k < k_F \quad (10a) \\ \dfrac{\hbar^2 k^2}{2m} + E_g, & k > k_F . \quad (10b) \end{cases}$$

Since this model represents a drastic simplification of the actual band structure, the "band gap" E_g is most properly thought of as an adjustable parameter. It is chosen such that the value of the static dielectric constant is correct for the material in question. In the present work the value is set equal to 4.8 eV for Si as in Ref. [11], which uses the same approximations. Having prescribed $E(\mathbf{k})$ one may readily evaluate the imaginary component of $\epsilon_{0,0}$. The real component may then be obtained from the appropriate Kramers-Kronig relation. The resulting expressions are algebraically complicated and it is not instructive for them to be displayed here.

Let us now consider some simplifications that become possible when applying these results to high-energy cases, where the particle is fully ionized. It was shown by BKK [11] that under these conditions (along with some additional simplifying assumptions) the above formulas for stopping power may be reduced to simple analytic expressions. They have reported that for velocities v such that $v \gg v_F$, where v_F is the Fermi velocity of the target electron distribution, the stopping power may be determined from

$$S(0) = \frac{Z_1^2 e^2 \omega_p^2}{v^2}\ln\left[\frac{2mv^2}{\hbar\omega_p}\right] \quad (11)$$

and

$$S(\mathbf{G}) = \frac{Z_1^2 e^2 \omega_p^2}{v^2} f(\mathbf{G})\ln\left[\frac{2mv}{\hbar G}\right] , \quad (12)$$

where m is the electron mass, $\omega_p^2 = 4\pi e^2 n/m$ is the plasma frequency, and n is the electron density. These formulas have displayed good agreement with experiment for low-Z_1 ions at very high energies [11]. In the following section, results obtained from the above formulas are compared with the present work for velocities $v \gtrsim v_F$. Comparisons in the low end of this velocity range must be judged cautiously, however, since these formulas are not expected to be valid in that region.

We now turn to the question of evaluating the proportion of the different charge-state species for ions traveling through matter. Our starting point for this is a Bohr electron-stripping criterion [23–25]. Using this model one postulates that for the bound electrons the smallest orbital velocity is proportional to the relative velocity of the ion and the Fermi velocity of the electrons in the medium. Formally, if the orbital velocity v_{orb} of an electron is such that $v_{\mathrm{orb}} \lesssim b v_{\mathrm{rel}}$, then that electron is considered to be unbound. The parameter b is referred to as the stripping parameter and its value is known to be of order unity [25]. The expressions for the relative velocity of the traveling ion and the target electron Fermi velocity have been given by Kreussler, Varelas, and Brandt [26].

As mentioned above, in the present work we are concerned with the average equilibrium charge state of the helium ion in Si due to the singly and doubly ionized states. For simplicity charge-changing events are not included. In the case of singly ionized helium in the ground state the bound electron is described by a 1s-type wave function. The orbital angular momentum of this electron is quantized according to $mv_{\mathrm{orb}} r = \hbar$, where r is the radial coordinate of the electron in the spherically symmetric 1s state. From this one has a simple means to relate the orbital radius with its velocity. Therefore, if one requires that $v_{\mathrm{orb}} > b v_{\mathrm{rel}}$ in order for the electron to be bound to the nucleus then one may determine a critical distance r_{crit}, over which the orbital must be confined, viz.,

$$r_{\mathrm{crit}} = \frac{\hbar}{m b v_{\mathrm{rel}}} . \quad (13)$$

Thus any 1s electron for which $r > r_{\mathrm{crit}}$ is considered to be unbound and hence a simple energy-dependent ionization criterion is obtained.

Having established a critical distance in the manner described above, a statistical estimate of the ionization state may be obtained. As mentioned above, the polarization of the media screens the field of the moving ion. An electron therefore interacts with the ion nucleus through a screened Coulomb potential. Consequently,

the electron orbital radius is expanded somewhat relative to its value in a vacuum. Starting with a hydrogenic $1s$ wave function, Ferrell and Ritchie [27] and Kaneko [9] have used variational methods to describe the effect. For simplicity, in the present work this screening effect on the He^+ state is not included. Thus the electron density for He^+ in the ground state may be written as $|\psi_{1s,Z=2}(r)|^2$, where $\psi_{1s,Z=2}(r)$ is the electron wave function in a vacuum. Under the assumptions outlined above the fractional charge $C(v,b)$ that remains bound is given by

$$C(v,b)=4\pi\int_0^{r_{\rm crit}}|\psi_{1s,Z=2}(r)|^2r^2dr\ . \tag{14}$$

The ionization state $Q(v,b)$ of the helium ion is therefore

$$Q(v,b)=2-C(v,b)\ . \tag{15}$$

One may notice immediately that Eq. (15) has the physically correct upper and lower limits with respect to energy for He^+ incident on Si, namely, $\lim_{v_{\rm rel}\to\infty}Q(v_{\rm rel},b)=2$ and $\lim_{v_{\rm rel}\to 0}Q(v_{\rm rel},b)=1$. Since only the two charge-state species are considered, He^+ and He^{2+}, the relative proportion of each may be determined uniquely from a knowledge of $Q(v,b)$. The stopping power for either the single or double plus charge state may be obtained from Eq. (9) with the appropriate charge-density function $\rho_{ne}(\mathbf{q})$. Thus by knowing the relative charge-state populations and the associated stopping powers of each, the total stopping power as a function of energy is obtained from a linear combination.

III. RESULTS

We turn now to application of the methodology outlined in Sec. II. To illustrate the method, our results are compared with the experimental work of Eisen *et al.* [28]. Before proceeding to this comparison some details of the calculations are discussed.

Regarding the evaluation of $S(\mathbf{G})$, multiple Gaussian quadratures are used to evaluate the necessary triple integrals. The integrand appearing in Eq. (9) is well behaved except where $\epsilon_{0,0}=0$. The latter is the well-known condition for the existence of collective oscillation modes, the details of which have been discussed extensively in the literature (e.g., Ref. [19]), so it is mentioned only briefly here. Such effects exist only over a limited range of wave vectors (generally, $q\le q_{\rm crit}\sim\omega_p/v_F$). For a collective mode $\mathrm{Re}(\epsilon_{0,0})=\mathrm{Im}(\epsilon_{0,0})=0$ and to first order one finds

$$\mathrm{Im}\left[\frac{1}{\epsilon_{0,0}}\right]_{\rm plasmon}=-\frac{\pi}{\left[\dfrac{d\,\mathrm{Re}\epsilon_{0,0}}{d\omega}\right]_{\omega=\omega_k}}\delta(\omega-\omega_k)\ , \tag{16}$$

where ω_k is such that $\epsilon_{0,0}(q,\omega_k)=0$ for $q<q_{\rm crit}$. In evaluating the stopping power from Eq. (9) the plasmon contribution to the wave-vector integral can be dominant in some cases. This can be seen directly through a calculation of the plasmon contribution to the standard f-sum rule

$$\frac{-2}{\pi\omega_p^2}\int_0^\infty\omega\,d\omega\,\mathrm{Im}\left[\frac{1}{\epsilon_{0,0}(q,\omega)}\right]=1\ , \tag{17}$$

which is shown in Fig. 1 [both the above sum rule and its counterpart obtained from (8) are discussed in detail in Ref. [19]]. Below the threshold wave vector $q_{\rm crit}$ the contribution is evidently large. For $q>q_{\rm crit}$, on the other hand, the collective modes are damped out and only the single-particle excitations occur. Hence in Fig. 1 the relative plasmon contribution vanishes in this case. This information is useful in understanding the behavior of the wave-vector integrand in Eq. (9) and illuminates the underlying physics. It is also of interest to note that the sum rule requires the plasmon pole $\omega_k(q)$ to be accurately specified. A simple estimate of $\omega_k\simeq\omega_p$ is not sufficient and leads to a strong violation of Eq. (17). For the energy loss the magnitude of the threshold frequency qv determines the energy at which the plasmons contribute to the stopping power. In the $v\to\infty$ limit the sum rule (17) is instrumental in arriving at the analytic formulas [11] given in Eqs. (11) and (12). Examples of plasmon contribution to the total energy loss as a function of energy have been given elsewhere, for example, in Refs. [14,27].

Once having obtained the stopping-power Fourier components from Eq. (9), the application to the case of ions traveling in a well-defined crystallographic direction is considered. The necessary structure factors for Si that we use are obtained from the work of Vinsome and Jaros [29]. The $S(\mathbf{G})$ are evaluated for particles traveling down the midaxial positions, which are the so-called best channeled ions. We shall return to this point later when discussing the comparison of our results with experimental data.

Proceeding in the manner described above, the stopping power is evaluated for both the singly and doubly charged helium ions channeling in various directions. In order to calculate the net stopping power, however, one must determine the populations of the two charge states. This is calculated from the value of $Q(v,b)$ as given in Eq. (15). Figure 2 shows a plot of the ionization-state function $Q(v,b)$ for helium as a function of energy for several choices of the electron-stripping parameter b. Clearly, the high- and low-energy limits are 2 (i.e., full

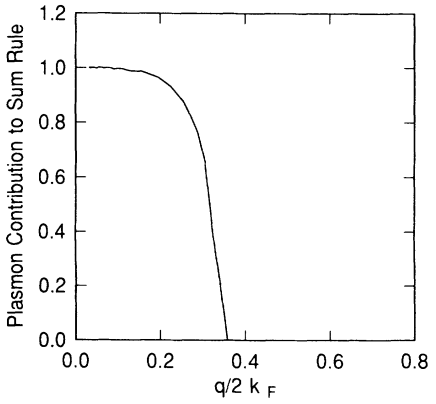

FIG. 1. The contribution to the sum rule Eq. (17) due to the plasmon modes.

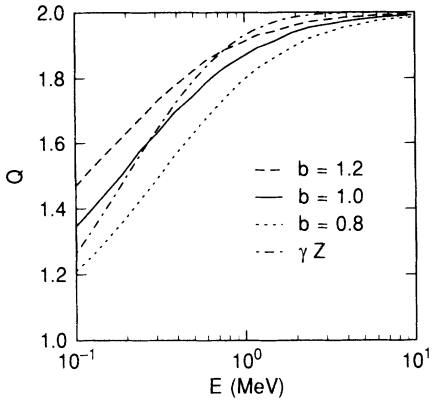

FIG. 2. The ionization function $Q(v,b)$ given by Eq. (15) as a function of energy and γZ calculated from Eq. (18).

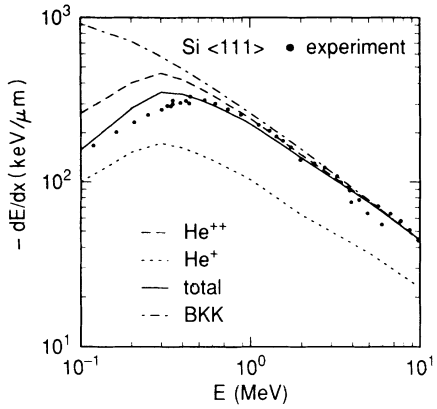

FIG. 3. Stopping power corresponding to the best channeled He ions in Si⟨111⟩. The curve labeled total represents a superposition of the results for He^{+} and He^{2+} (shown separately) as determined from the function $Q(v,1)$. The dashed-dotted line shows the corresponding result obtained using Eqs. (11) and (12) taken from Ref. [11]. The experimental data are taken from Ref. [28].

ionization) and 1, respectively, for any choice of b. In essence, the value of b is related to the effectiveness with which the medium removes a bound electron from a He ion having energy E. Later, the effect of b on the calculation of total stopping power is displayed. For now it is sufficient to comment that there is no rigorous choice for its value but that satisfactory results are obtained as long as b is chosen to be near to unity, as suggested in Ref. [25].

In studying the transmission of He^{+} ions through silicon, Williamson, Boujot, and Picard [30] introduced an effective charge-state parameter $Z^{*}=\gamma Z$, where

$$\gamma=\tanh[137\sqrt{(\pi/2)}v/(cZ)] \ . \tag{18}$$

For comparison, Fig. 2 shows the effective charge as calculated from Eq. (18) along with those determined from the Bohr stripping criterion using different values of the parameter b. The figure indicates a similar trend from both types of calculation, with the former showing a slightly faster increase in charge state as a function of energy. Equation (18) may also be used to resolve the fraction of singly and doubly charged ions at a given energy. Results for the total stopping power obtained using this are discussed below.

Figure 3 shows the results of a comparison between the present work and experimental data taken from Eisen *et al.* [28] for the best channeled ions in Si⟨111⟩. Experimentally, this corresponds to deducing the stopping power from the leading edge of the energy spectra for the transmitted beam. For ⟨111⟩, however, there is practically no difference between results obtained from leading edge and peak values of the energy spectra [28], since the channel electron density is only mildly inhomogeneous. For this calculation we choose to set $b=1$. The variation of this parameter is discussed separately below. Also shown in Fig. 3 are the resulting stopping powers for He^{2+} and He^{+} separately as function of energy. The solid line labeled "total" represents a superposition of the two results taken in a proportion determined from the function $Q(v,b)$. In the high-energy limit the projectile is expected to become fully ionized and therefore one finds that the curves for total and He^{2+} nearly coincide. In the opposite limit, toward zero energy, one would expect an incident He^{+} ion not to change its charge state. Therefore, one expects the total to coincide with the singly ionized results under these circumstances. It can be seen from Fig. 1, however, that even at 100 keV there is a substantial mixing of the two charge states. Stopping powers for energies smaller than this value have not been calculated since there does not exist any data suitable for a comparison in this energy range. The uppermost curve in Fig. 3 shows the stopping power obtained from Eqs. (11) and (12), which corresponds to the doubly ionized case [11]. Clearly, these equations can be properly used only past ~ 1 MeV, which corresponds to $\sim 3.3v_F$, where v_F is the Fermi velocity of target electrons.

It was mentioned above that the calculation for the total stopping power in Fig. 3 was obtained using a stripping parameter of $b=1$. Figure 4 shows results obtained using values of b equal to 1 and 0.8, as well as γZ from Eq. (18). We comment that in each case one obtains re-

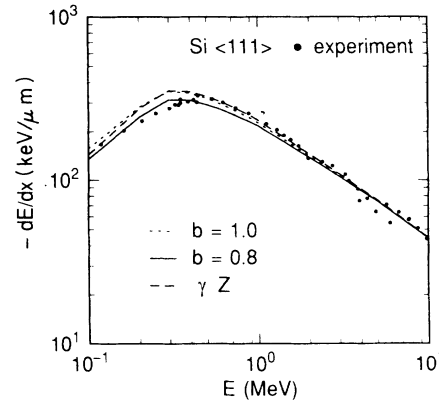

FIG. 4. Variation of the stripping parameter b. The various curves represent the total stopping power as in Fig. 3, as determined from the function $Q(v,b)$. The experimental data are taken from Ref. [28].

sults that remain in reasonable agreement with experiment. The largest spread in the results obtained from the two different values of b occurs at 100 keV where the values are 156 and 134 keV/μm for $b=1$ and 0.8, respectively. We conclude that the variation b in the neighborhood of unity gives rise to only modest shifts in the resulting curve and that these results are very similar to the result obtained independently from Eq. (18). Such uncertainties are inherent to the approach as there is no rigorous means to determine the value of b. It is worthwhile to note, however, that the experimental results themselves show uncertainties (random errors) of comparable magnitude.

In Fig. 5 the same type of comparison as was presented in Fig. 3 is shown, but for the case of He ion channeling in Si$\langle 110\rangle$. The experimental data [28] shows the stopping power as inferred from both the peak and the leading edge of the energy spectra for the transmitted beam. Since our calculations have been carried out for channeling along the midaxial paths, one would expect them to correspond to the stopping power inferred from the leading-edge data. In the case of $\langle 110\rangle$ there is a noticeable difference between the two sets of experimental data. For $\langle 111\rangle$, on the other hand, both are nearly the same and only the leading-edge data was shown in Fig. 3. Regarding the choice of b we note that since it is related to the effectiveness with which electrons are removed from the traveling ion, one might expect its value to be lower in $\langle 110\rangle$ than in $\langle 111\rangle$, where the electron density is much higher. In this spirit, we have adjusted the value of b from 1 (as used in Fig. 3) to 0.7, which produces a better overall fit to the experimental data. A very similar result is obtained by using the γZ given by Eq. (18) to calculate the total stopping power. As in Fig. 3, at sufficiently high energy the BKK result converges to the He^{2+} stopping-power curve as expected. The result shown in Fig. 5 is qualitatively similar to that shown in Fig. 3 but the stopping-power values throughout the same range in energy are noticeably smaller. The largest

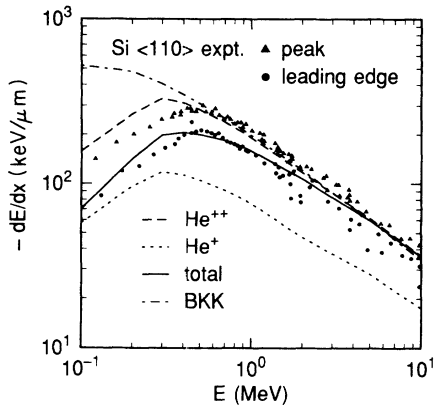

FIG. 5. Stopping power corresponding to the best channeled He ions in Si$\langle 110\rangle$. The curve labeled total represents a superposition of the results for He^+ and He^{2+} (shown separately), as determined from the function $Q(v,0.7)$ (see text). The dashed-dotted line shows the corresponding result obtained using Eqs. (11) and (12) taken from Ref. [11]. The experimental data are taken from Ref. [28].

source of discrepancy lies in the positions at which the stopping-power curve displays a maximum.

It is instructive to compare the results obtained above for the $\langle 111\rangle$ and $\langle 110\rangle$ axial channels with the corresponding results for the uniform electron gas. The latter corresponds to retaining only the $S(0)$ term in Eq. (9). In the case of $\langle 111\rangle$ the only non-negligible contribution to the electron-density nonuniformity comes from the $\{220\}$ set of Fourier components. The $\{220\}$ structure factors are much smaller then $f(0)$ [29]. Therefore the results for the uniform gas differ only slightly from those corresponding to $\langle 111\rangle$. This being the case, experimental stopping-power data for the $\langle 111\rangle$ channel is often compared with calculations based on the uniform gas term $S(0)$ [11]. In the present example, results for total stopping power using just $S(0)$ are found to be larger than those for $\langle 111\rangle$ by about $\sim 4\%$ at 100 keV, $\sim 6\%$ at 1 MeV, and $\sim 8\%$ at 10 MeV. One would therefore find a plot of $S(0)$ versus E to be almost coincident with the corresponding plot for the $\langle 111\rangle$ channel. In contrast, for the case of $\langle 110\rangle$, many sets of $\{hkl\}$ terms are effective in modifying the electron density in the channel. One can immediately see from a comparison of Figs. 3 and 5 that the difference between the $S(0)$ and $\langle 110\rangle$ results is substantial. Actual calculations show that the total stopping power calculated from just $S(0)$ is larger than the $\langle 110\rangle$ case by about $\sim 28\%$ at 100 keV, $\sim 32\%$ at 1 MeV, and $\sim 57\%$ at 10 MeV.

IV. CONCLUSION

We have presented calculations for stopping power of He in Si. Our calculations have explicitly included the contributions from singly and doubly ionized projectiles. For the case of He considered here the treatment of the singly ionized case is simplified through the use of an analytic approximation for the charge-density function. It is found that these calculations give reasonable agreement with experiment when superimposed using simple physical arguments for the ionization probabilities. For ions containing several electrons the corresponding charge densities can be obtained numerically from Hartree-Fock calculations.

The present work is a simplified treatment of the problem in that we have included the target valence-electron contribution only and restricted attention to channeling down the midaxial paths. For this reason comparing our results with experiment is most appropriate in the case where the latter is determined from the leading edge of the measured energy spectra. In the case of $\langle 111\rangle$ there is very little difference between the peak and leading-edge results so we have shown only those from the leading edge. In the $\langle 110\rangle$ case the difference between the two is much more pronounced as seen in Fig. 5.

Regarding a comparison between the calculated total and the experimentally determined stopping power, a few general comments can be made. The agreement is good except in the immediate vicinity of the stopping-power maximum. One notices that the calculated peak in $-dE/dx$ lies somewhat to the left of the experimental peak. Indeed, this a general feature that has been ob-

served in most stopping-power calculations (e.g., see Refs. [10,11,12]). The essential feature remains, however, that only a superposition of the results for different charge states is successful in replicating the experiment through the majority of the energy range considered. In the present case we demonstrate that even such a superposition made on simple grounds is reasonably successful in matching experiment.

ACKNOWLEDGMENT

The authors are grateful to Don Samuels for his help in digitizing the experimental data.

[1] H. A. Bethe, Ann. Phys. (Leipzig) **5**, 325 (1930).
[2] F. Bloch, Ann. Phys. (Leipzig) **16**, 285 (1933).
[3] J. Lindhard, M. Scharff, and S. Schiott, K. Dan. Vidensk. Selsk. Mat. Fys. Medd. **33**, No. 14, (1963).
[4] O. Firsov, Zh. Eksp. Teor. Fiz. **36**, 1517 (1959) [Soviet Phys.—JETP **36**, 1076 (1959)].
[5] P. Hvelplund and B. Fastrup, Phys. Rev. **165**, 408 (1968).
[6] N. Azziz, K. W. Brannon, and G. R. Srinivasan, Phys. Status Solidi B **142**, 35 (1987); N. Azziz and P. C. Murley, *ibid.* **151**, K105 (1989).
[7] W. Brandt and M. Kitagawa, Phys. Rev. B **25**, 5631 (1982).
[8] N. Azziz, K. W. Brannon, and G. R. Srinivasan, in *Ion Beam Processes in Advanced Electronic Materials and Device Technology,* edited by B. R. Appleton, F. H. Eisen, and T. W. Sigmon, MRS Symposia Proceedings No. 45 (Materials Research Society, Pittsburgh, 1985), p. 71.
[9] Toshiaki Kaneko, Phys. Rev. A **33**, 1602 (1986).
[10] A. Arnau, M. Penalba, P. M. Echenique, F. Flores, and R. H. Ritchie, Phys. Rev. Lett. **65**, 1024 (1990).
[11] A. F. Burenkov, F. F. Komarov, and M. A. Kumakhov, Phys. Status Solidi B **99**, 417 (1980).
[12] A. Desalvo and R. Rosa, J. Phys. C **10**, 1595 (1977).
[13] F. Bonsignori and A. Desalvo, J. Phys. Chem. Solids **31**, 2191 (1970).
[14] F. F. Komarov and M. A. Kumakhov, Radiat. Eff. **22**, 1 (1974).
[15] W. Brandt and J. Reinheimer, Can. J. Phys. **46**, 607 (1968); Phys. Rev. B **2**, 3104 (1970).
[16] F. Bonsignori and A. Desalvo, Lett. Nuovo Cimento **1**, 589 (1969).
[17] W. Both and J. S. Grant, Nucl. Phys. **63**, 481 (1965).
[18] F. J. Rogers, H. C. Graboske, Jr., and D. J. Harwood, Phys. Rev. A **1**, 1577 (1970).
[19] D. Pines, *Elementary Excitations in Solids* (Addison-Wesley, New York, 1963).
[20] D. S. Falk, Phys. Rev. **18**, 105 (1960).
[21] D. Penn, Phys. Rev. **128**, 2093 (1962).
[22] D. L. Johnson, Phys. Rev. B **9**, 4475 (1974).
[23] N. Bohr, K. Dan. Vidensk. Selsk. Mat. Fys. Medd. **18**, No. 8 (1948).
[24] H. D. Betz, Rev. Mod. Phys. **44**, 465 (1972).
[25] W. Brandt, in *Atomic Collisions in Solids,* edited by S. Datz, B. R. Appleton, and C. D. Moak (Plenum, New York, 1975), Vol. 1, p. 261.
[26] S. Kreussler, C. Varelas, and W. Brandt, Phys. Rev. B **23**, 82 (1981).
[27] T. L. Ferrell and R. H. Ritchie, Phys. Rev. B **16**, 115 (1977).
[28] F. H. Eisen, G. J. Clark, J. Bottinger, and J. M. Poate, Radiat. Eff. **13**, 93 (1972).
[29] P. K. W. Vinsome and M. Jaros, J. Phys. C **4**, 1360 (1971).
[30] C. F. Williamson, J. F. Boujot, and J. Picard, Centre d'Etudes Nucleares de Saclay Report No. R-3042, 1966 (unpublished).